Perylene π-Bridges Equally Delocalize Anions and Cations: Proportioned Quinoidal and Aromatic Content

Perylene π–Bridges that Equally Delocalize Anions and Cations: Quinoidal and Aromatic Contents in the Right Proportion

Paula Mayorga Burrezo[†] Wangdong Zeng,[†] Michael Moos, Marco Holzapfel, Sofia Canola, Fabrizia Negri,* Concepciò Rovira, Jaume Veciana, Hoa Phan, Jishan Wu,* Christoph Lambert, and Juan Casado*

Abstract: A complete experimental and theoretical study has been carried out for aromatic and quinoidal perylene-based bridges, either substituted with bis(diarylamine) or bis(arylimine) groups. The through-bridge inter-redox site electronic couplings (V_{AB}) have been calculated, for their respective mixed-valence radical cation and radical anion species. The unusual similitudes of the resulting V_{AB} values for the given structures reveal the intervention of molecular shapes with balanced semi-quinoidal/semi-aromatic structures in the charge delocalization. An identical molecular object equally responding to the injection of positive or negative charges is rare in the field of organic π–conjugated molecules. However, once probed herein for perylene-based systems, it can be extrapolated to others π–conjugated bridges. As a result, this work opens the door to the rational design of true ambipolar bulk and molecular conductors.

Organic mixed valence (MV)[1,2] molecules are key molecular models to test electron transfer theories in Chemistry, as well as for the conceptual design of new and more efficient wires for single molecular electronics.[3,4] The prototypical MV molecule is constituted by a conjugate bridge that connects two redox-active terminal groups, either oxidable donor groups or reducible acceptors. The MV property emerges in the monovalent species, either the radical cation or radical anion, due to the competition for the charge between the redox center. The electron/hole delocalization over the bridge depends on several factors, such as the nature of the redox-active groups or the bridge (i.e., length, conformation, composition, etc.) and of the surrounding medium (solvent, counterions, etc).[5–7] Regarding the terminal groups, if these are electron-acceptors, electrons are transferred in radical anions, while, if they are electron-donors, holes are transferred in radical cations. MV studies in molecular species with the same bridge and terminally substituted with donors or acceptors units have been thoroughly studied.[3–13] For both, groups with different redox strengths have been reported.

Remarkably, to the best of our knowledge, no studies of hole stabilization in radical cations and electrons in radical anions have been carried out over the same bridge and between essentially the same terminal groups, such as highlighted in Scheme 1. This is a logical situation in MV compounds[3] since organic redox-active groups usually are either donors (i.e., bad acceptors) or acceptors (i.e., bad donors) but not simultaneously good for both. Another interesting aspect is the analysis of the distribution of charges when the MV compounds are of Robin-Day class III since they could enable to analyze the electron / hole charge delocalization within the same bridge & redox-groups. Hence, designing MV systems in which the capability of a same π–bridge with a similar behavior faced with electrons and holes (having all other factors almost equal, Scheme 1) is a current challenge.

Scheme 1. Radical cation and anion with identical bridges and very similar redox-active groups, ●G ≈ ●G' and +G ≈ -G'.

To cope with this task, dealing with inherently different starting neutral π–bridges, either aromatic or quinoidal compounds[14–18] (**1** and **2** in Scheme 2) has been the chosen approach. These structures are designed in such a way that upon oxidation of the aromatic-based compound (i.e., **1** → **1**$^{\bullet+}$ in Scheme 2) a partial quinoidization (or partial remaining aromatization) of the bridge is produced. Conversely, reduction of the quinoidal-based compound (i.e., **2** → **2**$^{\bullet-}$) affords the attainment of a partial aromatization (or partial remaining quinoidization), such as depicted in Scheme 2. Thus it might result in similar bridge structures for the radical cation and anion. Regarding the redox sites, bis(diarylamine) groups have been chosen as the electron donor groups to be attached to the neutral aromatic bridge (see synthetic details in Scheme S1 and Figures S1-S8). On the other hand, the neutral quinoidal core in **2** connects two bis(arylimine) groups (synthesis already reported)[19]. Such as shown in Scheme 2, similar characters on the two CN moieties are achieved after the oxidation of the aromatic bis(diarylamine) and reduction of the quinoidal bis(arylimine), i.e., half-amine in the radical cation or half-imine in the anion. All in all, with the MV property study of **1** and **2**, analogous semi-amine (semi-imine) and semi-quinoidal (semi-aromatic) structures are obtained for the delocalization of the charge through the perylene bridge, the role of which, linked to similar redox-active groups, in the intramolecular charge transport will be mainly addressed. Electrochemical, UV-Vis-NIR spectroelectrochemical and EPR studies together with quantum chemical calculations are reported.

[*] Prof. J. Casado
Department of Physical Chemistry
University of Malaga
Campus de Teatinos s/n, 229071 Malaga, Spain
E-mail: casado@uma.es
[*] Dr. P. Mayorga,[†] Prof. C. Rovira, Prof J. Veciana
Department of Molecular Nanoscience and Organic Materials
Institut de Ciència de Materials de Barcelona (ICMAB)/ CIBER-BBN
Campus Universitari de Bellaterra. 08193, Cerdanyola (Spain)
[*] Dr. W. Zeng,[†] Dr. H. Phan, Prof. J. Wu
Department of Chemistry,
National University of Singapore
3 Science Drive 3, 117543 Singapore (Singapore)

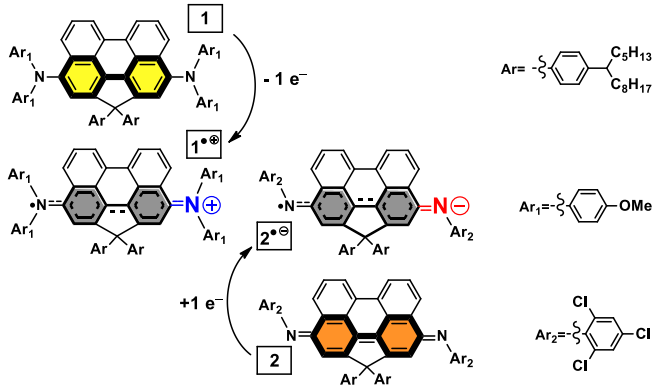

Scheme 2. Chemical structures of **1** and **2** and their MV radical cation (i.e., **1**$^{\bullet+}$) and radical anion (i.e., **2**$^{\bullet-}$) formed by oxidation and reduction, respectively.

Figure 1 depicts the electrochemical properties of **1** and **2**. Both display two reversible processes, anodic for **1** (Figure 1a) and cathodic for **2** (Figure 1b), leading to the consecutive generation of the radical cation (**1**$^{\bullet+}$) and dication in the first case, and of the radical anion (**2**$^{\bullet-}$) and dianion, in the second one. Small differences in electrochemical reversibility could be ascribed to the different experimental conditions in oxidation and reduction. Nonetheless, similar separations between each two processes (0.19 V for **1** and 0.16 V for **2**, Table S1 and S2 and Figures S9-S12) should be highlighted. To a large extent,[20] this energy should be that required to localize the two charges, either positives or negatives, into the terminal groups (due to repulsion energy) in the divalent forms. Hence, comparable differences between the redox potentials of both samples can be considered as a first hint of a similar nature of the π-conjugated bridge after the removal or addition of a single electron.

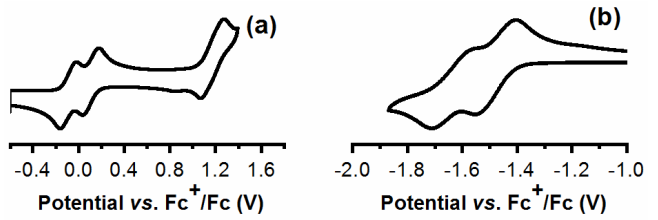

Figure 1. Cyclic voltammograms of **1** (a) and **2** (b) recorded at room temperature under Ar atmosphere (10^{-4} M/ 0.03 M TBA·PF_6/ *o*-DCB).

Encouraged by the reversibility and stability of the electrochemical processes, spectroelectrochemical UV-Vis-NIR absorption measurements were carried out for compounds **1**, under oxidation conditions, and **2**, under reduction ones (Figures 2a and 2c, respectively and Figures S13-S14). Progressive disappearance of the 544 nm band during oxidation of **1** was observed, giving way to the rise of two new absorptions at 846 and 1446 nm through isosbestic points.

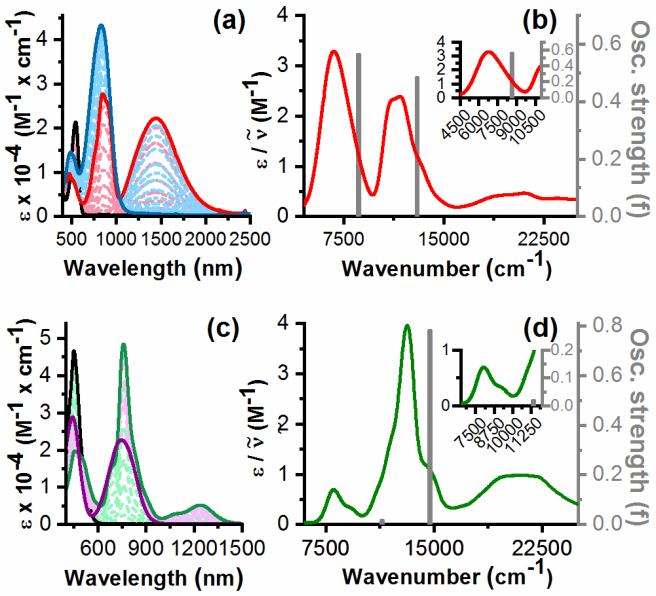

Figure 2. Electrochemically obtained (10^{-4} M/ 0.03M TBA·PF_6/ o-DCB) UV-Vis-NIR absorption spectra during oxidation of **1**: (a) neutral species, black solid line; radical cation, red solid line; dication, blue solid line, and reduction of **2**: (c), neutral species, black solid line; radical anion, green solid line; dianion, purple solid line. Additionally, the absorption spectra of **1**$^{\bullet+}$ (b) and **2**$^{\bullet-}$ (d) have also been included with their respective results from TD-UBLYP35/6-31G** calculations including o-DCB solvent described with PCM

Subsequent oxidation of **1**$^{\bullet+}$ yielded the dication, **1**$^{2+}$, which is characterized by one very strong band at 833 nm, completely dominating the UV-Vis-NIR absorption spectrum. This last feature is in good agreement with the appearance of a closed-shell quinoidal structures within the perylene unit between the two diarylamines in **1**$^{2+}$. Conversely, the reduction of **2** provoked the decrease of the band at 449 nm, accompanied by the increase of the bands at 760 and 1238 nm, related to the radical anion species, **2**$^{\bullet-}$. Posterior reduction of **2**$^{\bullet-}$ gave way to the appearance of a new band at 747 nm together with the one at 441 nm, ascribed to the dianion, **2**$^{2-}$, after the full clearance of the bands discussed for the radical anion.

Figure 2 also shows the reduced ($\varepsilon/\tilde{\nu}$) absorption spectra of the two pure radical species, **1**$^{\bullet+}$ (b) and **2**$^{\bullet-}$ (d), extracted from the spectroelectrochemical data. In both cases, a low-energy feature, that might be associated with the so-called intervalence charge transfer band (i.e., IV-CT band), was found. To further complement these experiments, DFT geometry optimizations of the neutral and charged species and TD-DFT calculations were performed (Figures S15-S17). As depicted in Figure 2 (b) and (d), a good theory-experiment matching was obtained. As expected, the dominant nature of the lowest excited state is the HOMO-1→HOMO for 1$^{\bullet+}$ and LUMO→LUMO+1 for 2$^{\bullet-}$, corroborating the assignment as the IV-CT band (Figure 3 and Figures S18-S19 and Table S4). Importantly, an equivalent contribution of both redox centers in each case was detected as clearly shown by the shape of the molecular orbitals shown in Figure 3. It is known that, in order to reach full delocalization among redox centers (i.e., a Robin–Day class III situation),[3] the V_{AB} must fulfill the 2 V_{AB} > λ_{AB} condition, with λ_{AB} as the intramolecular reorganization energy. According to a two-level model, for a Robin-Day class III situation, V_{AB} between the two redox centers can be evaluated as one half of the excitation energy of the IV-CT band.[4,6,7] Therefore, the assessment of the Robin-Day class, to which **1**$^{\bullet+}$ and **2**$^{\bullet-}$ belong,

became of fundamental importance. To this end, two approaches were adopted: first, we investigated the electronic communication between the bridge and the donor/acceptor groups by building an orbital interaction diagram (i.e., Figure 3). In this, each molecule was thought as the combination of two terminal donor (or acceptor) groups and a π-conjugated bridge represented by the perylene unit. Therefore, **1** was considered as a Donor-Bridge-Donor (DBD) system, while **2** responded to an Acceptor-Bridge-Acceptor (ABA) one. Accordingly, calculations were carried out on the full DBD or ABA molecules at their neutral optimized geometry and, separately, for the two fragments: the perylene fragment on one side and the dimer formed by two donor (or acceptor) groups, on the other side. As shown in Figure 3, a strong interaction occurred in **1** between the anti-symmetric combination of the two degenerate occupied orbitals of the two donor fragments and the HOMO orbital of the perylene fragment with a large contribution of the bridge to the HOMO and HOMO-2 of DBD. In this framework, the energy splitting provides an estimate of twice the coupling between the donor and the bridge[21] which is accordingly very large and matches an expected Robin Day class III system.

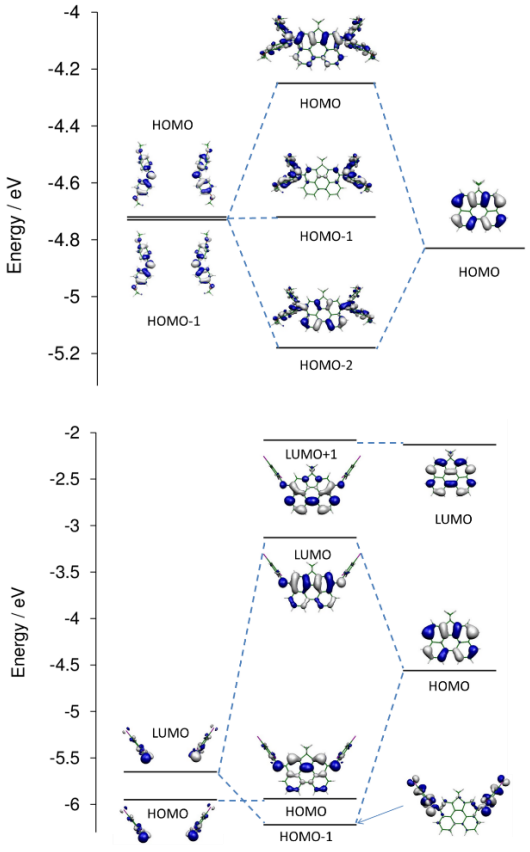

Figure 3. DFT//B3LYP/6-31G** orbital interaction diagrams for **1** (top) and **2** (bottom) between the two fragments (perylene bridge on the right, and donor dimer or donor acceptor dimer on the left).

A second approach, based on the determination of the optimized geometries of $\mathbf{1}^{\bullet+}$ and $\mathbf{2}^{\bullet-}$, was used. In both cases a delocalized distribution of the charge over the entire DBD or ABA system was revealed, in agreement with a class III. Indeed, Figure 3 shows that, in the case of $\mathbf{1}^{\bullet+}$, the initial state and the state created by the excitation from the HOMO-1 to the HOMO of DBD, determine the adiabatic + and – combination of the D^{+}-B-D and D-B-D^{+} localized diabatic states.[21] Thus, a correspondence of the HOMO-1→HOMO with the excitation into the IV-CT band was made. The V_{AB} was therefore estimated from the TD-UBLYP35 computed excitation energies (Tables S4-S5) of the IV-CT transition, resulting to be 4315 cm^{-1}. Same procedure was followed for **2** (Figure 3) whose orbital interaction diagram demonstrates a large electronic communication between the bridge and the acceptors. In this case, an interaction between the HOMO of perylene fragment and the antisymmetric combination of the unoccupied acceptor's orbitals occurs. Analogously to the DBD system, in $\mathbf{2}^{\bullet-}$, one-electron excitation from the LUMO to the LUMO+1 corresponds to the excitation into the IV-CT. The V_{AB} between the two redox centers, obtained with the same procedure as for **1**, amounts to ca. 5686 cm^{-1} (Table S4-S5). Interestingly, $\mathbf{1}^{\bullet+}$ is produced by extracting one electron from its HOMO by which its aromatic nature is reduced in favor of a quinoidal gaining. Conversely, $\mathbf{2}^{\bullet-}$ is produced by adding one electron into its LUMO which is also of aromatic nature by which the molecule gains a partial aromatic character in detriment of the quinoidal. Thus, both ions acquire a partial aromatic shape which turns out to be similar in extent.

Comparing the theoretical V_{AB} and λ_{AB} values of $\mathbf{1}^{\bullet+}$ and $\mathbf{2}^{\bullet-}$, λ_{AB} never exceeds 2500 cm^{-1} (Table S5), corroborating the class III MV assignment in both cases. Experimental V_{AB} values were also determined considering the energy of the IV-CT band (i.e., $\bar{\upsilon}_{max}$) from the UV-Vis-NIR spectra, by using $2V_{AB} = \bar{\upsilon}_{max}$. Asymmetric shapes of these IV-CT bands, typical of Class III MV behavior, were supported by double-peak fitting in $\mathbf{1}^{\bullet+}$ and $\mathbf{2}^{\bullet-}$ (Figures S20-S21 and Tables S6-S7). As a result, V_{AB} was set to 3464 cm^{-1} for $\mathbf{1}^{\bullet+}$ ($\bar{\upsilon}_{max}$ = 6928 cm^{-1}) and 4041 cm^{-1} for $\mathbf{2}^{\bullet-}$ ($\bar{\upsilon}_{max}$ = 8082 cm^{-1}) in good agreement with the theoretical values.

The generation of the class III MV species upon oxidation of **1** provokes the partial attainment of a quinoidal structure via emptying its HOMO orbital. Conversely, reduction of **2** proceeds by occupying the LUMO described as the combination of the empty LUMO orbitals of the arylimine groups with the HOMO of the perylene moiety. Consequently, charging in $\mathbf{1}^{\bullet+}$ produces the partial rupture of the aromatic shape of the bridge rings, while in $\mathbf{2}^{\bullet-}$ promotes an underlying partial aromaticity recovery of the rings of the bridge. This means that oxidation of **1** and reduction of **2** mix these two geometrical configurations very much in the same proportion (Figure S19, with the geometries of $\mathbf{1}^{\bullet+}$ and $\mathbf{2}^{\bullet-}$). In addition, a diarylamino group acquires a partial imine character upon oxidation, while reduction of the arylimine group induces an equivalent loss of its intrinsic character. The overall outcome is the adoption of very similar shapes in $\mathbf{1}^{\bullet+}$ and in $\mathbf{2}^{\bullet-}$, what translates into similar charge delocalization properties.

These certainly large V_{AB} values of $\mathbf{1}^{\bullet+}$ and $\mathbf{2}^{\bullet-}$ particularly that for $\mathbf{1}^{\bullet+}$, resulted to be among the largest found in the literature for bis(diarylamino) phenyl based compounds. For instance, it is somewhat smaller than that of bis(diarylamino) substituted benzene (benzene as a bridge, V_{AB} = 4765 cm^{-1}),[23] similar to a 2,6-substituted naphthalene derivative (3810 cm^{-1})[23] but larger as in the case of the biphenyl bridge (V_{AB} = 3180 cm^{-1}), where the coupling was evaluated as $V_{AB} = \bar{\upsilon}_{max}/2$ for comparison on an equal footing.[23] Unfortunately, the repertory of V_{AB} for radical anions is much more limited. However, the following cases of V_{AB} values for bis(nitroaryl) funcionalized[23,24] series can be mentioned: i) for benzene as a bridge, V_{AB} = 5410 cm^{-1}, for bis(nitroaryl) biphenyl radical anion, V_{AB} = 3400 cm^{-1}, and for the analogue with a naphthalene bridge, V_{AB} = 4250 cm^{-1}. In this context, the V_{AB} value for $\mathbf{2}^{\bullet-}$ fits also among the best obtained so far.[6,7] Figure 4 compiles the V_{AB} values of the above described

compounds together with those reported in this work. The simultaneous enlargement and rigidification of the π–bridge preferentially favor the delocalization of the anions compared to that of cations (i.e., notice the different condition regarding solvent and counterions).[6,7,23–25]. On the other hand, the difference between the V_{AB} values in **1**$^{\bullet+}$ and **2**$^{\bullet-}$ fall within the differences in the cases cited above. This is significant given that the amino and nitro derivatives are selected as good donor and acceptors, while the electroactive groups of **1**$^{\bullet+}$ and **2**$^{\bullet-}$ are selected on the basis their similarity rather than on their strengths.

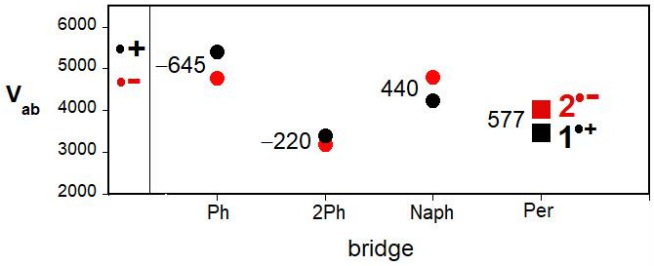

Figure 4. As filled circles: representation of the experimental V_{AB} for class III MV radical cations derived from bis(arylamino)phenylene (Ph), bis(arylamino)biphenyl (2Ph) and 2,6-bis(arylamino)naphthalene (Naph). As red circles: representation of the V_{AB} for class III MV radical anions derived from bis(nitroaryl)phenylene (Ph), bis(nitroaryl)biphenyl (2Ph) and bis(nitroaryl)naphthalene (Naph). As filled black and red squares are the values for **1**$^{\bullet+}$ and **2**$^{\bullet-}$, respectively. The $V_{AB(anion)}$– $V_{AB(cation)}$ values are inserted.

Longer π-conjugated bridges (i.e., quaterrylene and hexarylene units) with the same substitution pattern as **1** and **2** were also prepared (Scheme S1) and studied by electrochemistry (Figures S22-S23 and Tables S8-S9), UV-Vis-NIR spectroelectrochemistry (Figures S24, S27, S30 and S33) and quantum chemistry (Figures S25-S26, S28-S29, S31-S32 and S34-S35) and Figures S1-S8). Unfortunately, none of them could be analyzed in the context of MV framework due to a higher relevance of the central connecting bridge. In summary, oxidation of these enlarged bis(diarylamine) derivatives took place mostly on the central connecting bridge;[26] while in the case of the reduction of the bis(arylimine) series, a residual involvement of the arylimine groups was detected and the negative charge was preferentially stabilized on the quinoidal bridge.

Finally, Figure 5 shows the experimental and simulated EPR spectra of **1**$^{\bullet+}$ and **2**$^{\bullet-}$ recorded at low temperature (200 K). **1**$^{\bullet+}$ exhibits a five evenly spaced main lines[9,27] corresponding to the hyperfine coupling of the unpaired electron with two magnetically equivalent ^{14}N atoms with coupling constants of 0.32 mT. In the case of **2**$^{\bullet-}$, seven lines were found associated with the previously mentioned coupling of the unpaired electron with two magnetically equivalent ^{14}N atoms (a_N = 0.31 mT) and with the H atoms placed in the semi-quinoidal moiety (a_H = 0.22 mT) (Supporting Information, Figures S35-S36). These results evidence that, even at low temperature, the unpaired electron in both compounds is coupled with the two equivalent N atoms at both extremities of the molecule, in line with a fully delocalized structure or with a class III MV species, as already deduced from the discussion of theoretical and optical data.

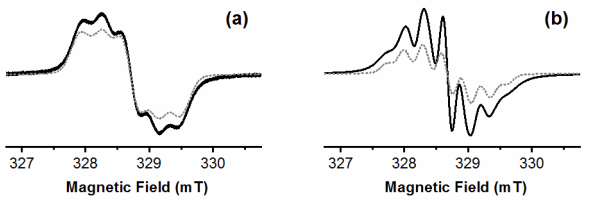

Figure 5. Electron paramagnetic resonance (EPR) spectra of **1**$^{\bullet+}$ (a) and **2**$^{\bullet-}$ (b) measured at 200 K under nitrogen atmosphere together with their simulated spectra (grey dotted lines). **1**$^{\bullet+}$ (g_e = 2.0031, 0.10 mM in DCM) was obtained by oxidation of a solution of **1** with 1 equiv of NO·SbF_6. In the case of **2**$^{\bullet-}$ (g_e = 2.0032, 0.20 mM in THF) the addition of 1 equiv of $CoCp_2$ was used.

In conclusion, it is commonly known that, in molecule-based electronic devices, the attainment of balanced (similar magnitudes) electron and hole mobilities is highly valuable. Therefore, it seems interesting to develop molecules that delocalize equally electrons or holes with similar extensions. This approach is rather new in the field due, in part, to the non-compatibility of a same redox-active organic being simultaneously good electron-donor and -acceptor and a same π–conjugated bridge to be “indifferent” in response to the delocalization of holes or electrons. Here, we have designed and probed the latter case, by preparing class III mixed valence systems of radical cation and radical anion of perylene-based aromatic and quinoidal bis(diarylamino) and bis(arylimine) bridges. The Marcus-Hush theory provides the electronic coupling values that allows us to conclude about the performance/efficiency of the resonance of the charge in the bridge between external groups. This work thus contributes with structure-function relationships to the development of redox ambipolar molecules. We show here that the molecular design for dual/balanced stabilization of electrons and holes in one molecule might put the focus in the electronic structure of the bridge and on its intermediate modulation along the quinoidal-to-aromatic interval. We are developing this concept with molecules with intermediate diradical character promoted by aromatic/quinoidal competition.

Acknowledgements

The authors are grateful for the financial support received from: MOTHER (MAT2016-80826-R) granted by the DGI (Spain), GenCat (2017-SGR-918) financed by DGR (Catalunya) and the Spanish Ministry of Economy and Competitiveness, through the “Severo Ochoa” Programme for Centres of Excellence in R&D (SEV-2015-0496) and through the project reference CTQ2015-69391-P and PGC2018-098533-B-100. M. B. gratefully acknowledges financial support from the Juan de la Cierva-Formación 2015 programme (FJCI-2015-23577) supported by MINECO and DAAD through the Research Grants- Short-Term Grants, 2017 programme (No: 91673720). J. W. thanks financial support from Ministry of Education Tier 3 program (MOE2014-T3-1-004). C. L thanks the Deutsche Forschungsgemeinschaft (DFG) for support within the GRK 2112.

Keywords: perylene • quinoidal • aromatic • charge delocalization • mixed valence

[1] J. Hankache, O. S. Wenger, *Chem. Rev.* **2011**, *111*, 5138–5178.

[2] B. S. Brunschwig, N. Sutin, *Coord. Chem. Rev.* **1999**, *187*, 233–254.

[3] M. B. Robin, P. Day, in (Eds.: H.J. Emeléus, A.G.B.T.-A. in I.C. and R. Sharpe), Academic Press, **1968**, pp. 247–422.

[4] N. S. Hush, *Coord. Chem. Rev.* **1985**, *64*, 135–157.

[5] J.-P. Launay, *Chem. Soc. Rev.* **2001**, *30*, 386–397.

[6] A. Heckmann, C. Lambert, *Angew. Chem. Int. Ed.* **2012**, *51*, 326–392.

[7] C. Lambert, in *Organic Redox Systems*, John Wiley & Sons, Inc, Hoboken, NJ, **2015**, pp. 245–268.

[8] S. Barlow, C. Risko, S. A. Odom, S. Zheng, V. Coropceanu, L. Beverina, J.-L. Brédas, S. R. Marder, *J. Am. Chem. Soc.* **2012**, *134*, 10146–10155.

[9] M. M. Hansmann, M. Melaimi, G. Bertrand, *J. Am. Chem. Soc.* **2018**, *140*, 2206–2213.

[10] B. R. Kaafarani, C. Risko, T. H. El-Assaad, A. O. El-Ballouli, S. R. Marder, S. Barlow, *J. Phys. Chem. C* **2016**, *120*, 3156–3166.

[11] P. M. Burrezo, N.-T. Lin, K. Nakabayashi, S. Ohkoshi, E. M. Calzado, P. G. Boj, M. A. Díaz García, C. Franco, C. Rovira, J. Veciana, et al., *Angew. Chem. Int. Ed.* **2017**, *56*, 2898–2902.

[12] D. E. Richardson, H. Taube, *J. Am. Chem. Soc.* **1983**, *105*, 40–51.

[13] S. F. Nelsen, *Chem. Eur. J.* **2000**, *6*, 581–588.

[14] T. M. Pappenfus, J. D. Raff, E. J. Hukkanen, J. R. Burney, J. Casado, S. M. Drew, L. L. Miller, K. R. Mann, *J. Org. Chem.* **2002**, *67*, 6015–6024.

[15] J. Casado, M. Z. Zgierski, P. C. Ewbank, M. W. Burand, D. E. Janzen, K. R. Mann, T. M. Pappenfus, A. Berlin, E. Pérez-Inestrosa, R. P. Ortiz, et al., *J. Am. Chem. Soc.* **2006**, *128*, 10134–10144.

[16] P. M. Burrezo, J. L. Zafra, J. T. López Navarrete, J. Casado, *Angew. Chem. Int. Ed.* **2017**, *56*, 2250–2259.

[17] Z. Zeng, M. Ishida, J. L. Zafra, X. Zhu, Y. M. Sung, N. Bao, R. D. Webster, B. S. Lee, R.-W. Li, W. Zeng, et al., *J. Am. Chem. Soc.* **2013**, *135*, 6363–6371.

[18] Z. Zeng, S. Lee, J. L. Zafra, M. Ishida, X. Zhu, Z. Sun, Y. Ni, R. D. Webster, R.-W. Li, J. T. López Navarrete, et al., *Angew. Chem. Int. Ed.* **2013**, *52*, 8561–8565.

[19] W. Zeng, Y. Hong, S. Medina Rivero, J. Kim, J. L. Zafra, H. Phan, T. Y. Gopalakrishna, T. S. Herng, J. Ding, J. Casado, et al., *Chem. Eur. J.* **2018**, *24*, 4944–4951.

[20] Ion pairing especially in weakly polar solvent such as oDCB affects the redox potentials strongly. See for instance: R. Winter, *Organometallics* **2014**, *33*, 4517-4536.

[21] W. Jiang, C. Xiao, L. Hao, Z. Wang, H. Ceymann, C. Lambert, S. Di Motta, F. Negri, *Chem. Eur. J.* **2012**, *18*, 6764–6775.

[22] V. Coropceanu, N. E. Gruhn, S. Barlow, C. Lambert, J. C. Durivage, T. G. Bill, G. Nöll, S. R. Marder, J.-L. Brédas, *J. Am. Chem. Soc.* **2004**, *126*, 2727–2731.

[23] C. Lambert, G. Nöll, *J. Am. Chem. Soc.* **1999**, *121*, 8434–8442.

[24] S. F. Nelsen, A. E. Konradsson, M. N. Weaver, J. P. Telo, *J. Am. Chem. Soc.* **2003**, *125*, 12493–12501.

[25] S. F. Nelsen, M. N. Weaver, J. I. Zink, J. P. Telo, *J. Am. Chem. Soc.* **2005**, *127*, 10611–10622.

[26] S. Rodríguez González, M. C. Ruiz Delgado, R. Caballero, P. De la Cruz, F. Langa, J. T. López Navarrete, J. Casado, *J. Am. Chem. Soc.* **2012**, *134*, 5675–5681.

[27] Y. Li, K. C. Mondal, P. P. Samuel, H. Zhu, C. M. Orben, S. Panneerselvam, B. Dittrich, B. Schwederski, W. Kaim, T. Mondal, D. Koley, H. W. Roesky, *Angew. Chem. Int. Ed.* **2014**, *53*, 4168–4172.